

Bayesian modelling of repeated measures lung function data from multiple-breath washout tests

Robert K Mahar^{1,2} , John B Carlin^{1,2,3}, Sarath Ranganathan^{2,4,5}, Anne-Louise Ponsonby^{2,6}, Peter Vuillermin^{2,6,7}, and Damjan Vukcevic^{1,8,9}

1. Data Science, Murdoch Childrens Research Institute, Parkville, Victoria, Australia
2. Department of Paediatrics, Faculty of Medicine, Dentistry and Health Services, University of Melbourne, Parkville, Victoria, Australia
3. Melbourne School of Population and Global Health, Faculty of Medicine , Dentistry and Health Services, University of Melbourne, Parkville, Victoria, Australia
4. Infection and Immunity, Murdoch Childrens Research Institute, Parkville, Victoria, Australia
5. Department of Respiratory and Sleep Medicine, Royal Children's Hospital, Parkville, Victoria, Australia
6. Population Health, Murdoch Childrens Research Institute, Parkville, Victoria, Australia
7. School of Medicine, Faculty of Health, Deakin University, Geelong, Victoria, Australia
8. School of Mathematics and Statistics, Faculty of Science, University of Melbourne, Parkville, Victoria, Australia
9. School of BioSciences, Faculty of Science, University of Melbourne, Parkville, Victoria, Australia

Corresponding author: Damjan Vukcevic, Data Science, Murdoch Childrens Research Institute, Flemington Road, Parkville, 3052. Ph: +61 3 9936 6567. Email: damjan.vukcevic@mcri.edu.au

Keywords: lung clearance index, multiple-breath washout, linear mixed models, modelling, incomplete data.

Abstract

Paediatric respiratory researchers have widely adopted the multiple-breath washout (MBW) test because of its ability to assess lung function in unsedated infants and because it is well suited to the longitudinal study of lung development and disease. However a substantial proportion of MBW testing cycles in infants produce data that fail to meet the current acceptability criteria and novel analytic approaches are required. MBW test results in current practice are simple empirical summaries of observed gas-volume cycles, yet the data have a clear underlying functional form that suggests a model-based approach may be valuable. We present a novel statistical model for infant MBW data and apply it to 1,197 tests from 432 individuals from a large birth cohort study. We focus on Bayesian estimation of the lung clearance index (LCI), the most commonly used summary of lung function from MBW tests. This approach allows us to directly quantify uncertainty in our estimates and to incorporate prior information into our analyses. Our results show that the model provides an excellent fit to the data and leads to similar estimates to the standard empirical approach. Furthermore, it enables LCI to be estimated using tests with different degrees of completeness, something not possible with the standard approach. Our model therefore allows previously unused data to be used rather than discarded, as well as routine use of shorter tests without significant loss of accuracy. This will in turn lead to larger effective datasets from fixed cohort samples and greater feasibility of clinical use.

Introduction

Chronic adult diseases, and respiratory diseases in particular, often have their origins in early life, and lung function in these early years is a major determinant of lung function in later life [1]. The human lung undergoes rapid development while in utero, continuing up until late infancy and, in some cases, well beyond that. Adverse lung growth and development during gestation and infancy has been associated with lifelong deficits in lung function and respiratory health. In this context, techniques are required that enable accurate and feasible measurement

of lung function across the life course to better monitor disease progression and manage responses to therapeutic interventions [2, 3].

The inert gas multiple-breath washout (MBW) test is increasingly used to measure lung function in individuals with chronic and serious lung diseases such as cystic fibrosis (CF), as well as in cohort studies investigating the early life origins of asthma and chronic obstructive pulmonary disease. Recent clinical trials have also adopted the MBW as a primary tool to monitor patient responses to therapeutic interventions [4]. The test begins with a 'wash-in' phase: a mouthpiece and nose clip are fitted to the patient and, after several breaths of room air, the patient starts inhaling an inert tracer gas mixture until the concentration of inert gas is in equilibrium. At this point, the patient is switched back to room air and the 'washout' phase of the test commences. The molar mass of the respired gases and airflow are measured over the washout at high frequency until the lungs are effectively clear of the tracer gas. Specialised software then performs breath detection and derives various quantities that are used to assess lung function. Crucially, the washout phase of the test must be performed during regular, uninterrupted breathing.

The use of MBW in young children is favoured over more conventional lung function tests such as single-breath washout and spirometry, since it requires minimal patient co-operation and co-ordination [5, 6]. While lung function can be assessed by a number of different summaries of the MBW test, the most commonly used is the lung clearance index (LCI) [7] which is based on the functional residual capacity (FRC), a widely used measure of lung function in its own right. The widespread adoption of the MBW has culminated in a recent consensus statement that recommends guidelines for MBW analysis and highlights areas that need further research [5].

The data captured during an MBW test and used to calculate the LCI suggest an underlying functional form, yet to our knowledge no one has thus far used an explicit statistical model to exploit this. The standard method for calculating LCI instead uses a simple algorithm based on the observed values [5]. By not modelling the underlying process, the standard method does not

in general fully exploit the available information. We propose a relatively simple stochastic model for MBW data that leads to a model-based definition of the LCI. Our approach explicitly models the quantities used to calculate LCI, namely the cumulative expired volume (CEV) and FRC. Based on these explicit definitions of the estimands for LCI, CEV, and FRC, we develop a Bayesian estimation method.

One immediate and novel application of this model is to estimate LCI and FRC from incomplete or shortened MBW datasets. Shortening the test procedure is of practical interest because it is time-consuming and prone to disruption, particularly in patients with advanced disease, in preschool children who have shorter attention spans, and among infants who are being tested during natural sleep. In some cases, breathing irregularities during the wash-in, such as sighs, can sometimes be acceptable [8]. If breathing irregularities occur during the washout or the patient becomes unsettled, the test data are typically not used and additional testing must be performed or testing abandoned. Indeed in most studies conducted among sleeping babies, successful MBW measures have only been obtained in 60-70% of tested participants. One way the MBW procedure can be shortened is by terminating the test early. A number of recent studies have shown that, under certain circumstances, MBW tests can be substantially shortened while still providing clinically meaningful results [9-11]. These studies represent important innovations to the MBW technique and cast doubt on whether the test must be complete before a meaningful summary statistic can be derived. However, they do this by defining a different type of LCI which is only informative of earlier timepoints in the test. In contrast, our approach is to model the available shortened test data, allowing us to extrapolate it out to directly estimate the usual LCI.

Using data from a large birth cohort study, we assess how our model-based method of estimating LCI, CEV, and FRC compares to the standard method using complete MBW tests. We then assess the performance of our model-based method with shortened MBW tests.

We adopt a Bayesian modelling approach as it allows us to naturally incorporate prior information and account for uncertainty in estimation of our model parameters. By assigning prior distributions to model parameters we are also able to constrain them to more realistic values, which we show is particularly helpful when analysing incomplete tests. We use a large dataset of tests in normal infants to estimate an appropriate informative prior and validate its use.

Methods

Data

The Barwon Infant Study (BIS) is a birth cohort study in the Barwon region of south-eastern Australia designed to investigate the impact of early-life exposures on immune, allergic, cardiovascular, respiratory, and neurodevelopmental outcomes ($n = 1,074$) [12].

MBW data were collected from infants aged between 4 and 12 weeks between February 2011 and December 2013. Acceptable tests exhibited a stable breathing pattern with no artefacts such as sighs, sucking, snoring, or mask leaks, or any observable software artefacts. We obtained a total of 1,197 acceptable MBW tests from 432 infants in this study. Of these infants, 89 (21%) had only a single test performed, while 115 (27%), 98 (23%), 81 (19%), 35 (8%), 13 (3%), and 1 (<1%) participants had 2, 3, 4, 5, 6, and 7 replicate measurements available, respectively. MBW tests were performed in accordance with current guidelines [5]. Infants were tested during natural sleep. All tests were performed with 4% sulphur hexafluoride (SF_6) using a mainstream ultrasonic flowmeter (Exhalyzer D, Ecomedics, Duernten, Switzerland). For the purposes of this analysis, MBW data were processed with WBreath (version 3.19, ndd Medizintechnik AG, Zurich, Switzerland). Use of the WBreath graphical user interface was automated using AutoIt, a scripting language [13].

Modelling MBW data

The data collected as part of a routine MBW test consist of air flow (L/s) and molar mass of the gas mixture (g/mol) measured over a short period of time (approx. 1–3 min) at high frequency (200 Hz) using an ultrasonic flowmeter (see Figure 1). The wash-in component of the test is not typically of interest and is thus discarded. From the subsequent wash-out phase of the test, the following quantities are derived (see Figure 2): the tracer gas quantity (the current amount of tracer gas, as a proportion of the amount of tracer gas at the start of the washout) (GAS), cumulative expired volume of gas mixture (CEVGM), and the cumulative expired volume of tracer gas (CEVTG). As is typically done, we derive discrete versions of these by calculating them on a per-breath basis (the quantities are therefore interpretable as representing the state at the end of each breath cycle) [5, 14].

We first introduce notation for modelling the data from a single MBW test. Let k ($k = 0, 1, 2, \dots, K$) index breaths from the start of the washout phase (indexed by $k = 0$). We denote the GAS, CEVGM, and CEVTG series as $c(k)$, $v(k)$, and $r(k)$ respectively. Figure 2 shows $c(k)$, $v(k)$, and $r(k)$ for 10 randomly selected MBW tests. The LCI as defined in the aforementioned consensus statement, herein referred to as the ‘standard method’, is denoted here as

$$LCI^{(s)} = \frac{CEV^{(s)}}{FRC^{(s)}} = \frac{v(k^{(40)})}{r(k^{(40)}) / (1 - c(k^{(40)}))}, \quad (1)$$

where the cumulative expired volume ($CEV^{(s)}$) denotes the CEVGM measured at breath $k^{(40)}$, the functional residual capacity ($FRC^{(s)}$) denotes an estimate of the volume of a typical expiration (using quantities measured at breath $k^{(40)}$), and the parenthetical s denotes the ‘standard method’. As recommended in the consensus guidelines [5], the $k^{(40)}$ used to calculate the quantity in equation (1) is the first of three consecutive breaths for which $c(k) \leq 1/40$. We define a complete test to be one that allows identification of $k^{(40)}$; i.e. it must include data measured up to the third consecutive breath for which $c(k)$ is under $1/40$.

Our approach was to specify statistical models for $c(k)$, $v(k)$, and $r(k)$, with each quantity represented by a smooth function plus independent random error.

We modelled the tracer gas quantity $c(k)$ using a two-phase exponential decay function of k , which is implied by a theoretical two-compartment lung model [15]:

$$f(k; \gamma) = \gamma_0 e^{-\gamma_1 k} + (1 - \gamma_0) e^{-\gamma_2 k}, \quad (2)$$

where $0 < \gamma_0 < 1$ is the proportionate weight of the fast decaying component and γ_1 & γ_2 ($0 < \gamma_1 < \gamma_2$) denote the fast and slow decay constants respectively. This model is commonly applied to various physical systems, including the lungs, and at least one recent study has applied the model directly to MBW end-tidal tracer gas concentration in adults, albeit to achieve different aims [16]. Since the data are restricted to be positive, we model c as log-normal with independent and identically distributed errors:

$$c(k) \sim \log N(f(k; \gamma), \sigma_c). \quad (3)$$

The cumulative expired volume of gas mixture, $v(k)$, was modelled as an increasing linear function of k , with geometric mean

$$g(k; \alpha) = \alpha k, \quad (4)$$

and the cumulative expired volume of tracer gas, $r(k)$, as an increasing exponential decay function of k , with geometric mean

$$h(k; \beta) = \beta_0 (1 - e^{-\beta_1 k}). \quad (5)$$

Note that the functions v and r are both strictly positive and monotonically increasing, which we capture by modelling their discrete derivatives (denoted here with primes), and do so on a log scale:

$$\ln(g'(k; \alpha)) = \ln(\alpha), \quad (6)$$

$$\ln(h'(k; \beta)) = \ln(\beta_0) + \ln(1 - e^{-\beta_1}) - \beta_1 k. \quad (7)$$

An added benefit of these transformations is that we can assume independent and identically distributed errors on a natural scale for each quantity, giving us the final model:

$$v'(k) \sim \log N(g'(k; \alpha), \sigma_v), \quad (8)$$

$$r'(k) \sim \log N(h'(k; \beta), \sigma_r). \quad (9)$$

Using this model, we define the end-test breath, which we denote θ , as the real-valued breath index at which the expected value of c is equal to 1/40:

$$\theta \equiv k : E(c(k)) = \frac{1}{40}. \quad (10)$$

We can thus redefine FRC, CEV, and therefore LCI, in terms of the model parameters:

$$CEV^{(m)} = g(\theta; \alpha), \quad (11)$$

$$FRC^{(m)} = \frac{h(\theta; \beta)}{1 - f(\theta; \gamma)}, \quad (12)$$

$$LCI^{(m)} = \frac{g(\theta; \alpha)}{h(\theta; \beta)/(1 - f(\theta; \gamma))}, \quad (13)$$

where the parenthetic m denotes the ‘model-based’ method. Note, however, that the standard method defines FRC in terms of a “sample statistic”, by taking the observed cumulative expired volume of tracer gas and dividing it by $1 - c(k)$ at breath $k^{(40)}$, where some gas will remain in the lungs. Using the model-based method a more natural approach is to use the asymptotic value of $FRC^{(m)}$, which represents the state of the lungs when completely free of the inert gas:

$$\lim_{k \rightarrow \infty} \frac{h(k; \beta)}{(1 - f(k; \gamma))} = \beta_0. \quad (14)$$

Thus we propose a more refined model-based definition, denoted by an asterisk, with $FRC^{(m^*)} = \beta_0$, giving:

$$LCI^{(m^*)} = \frac{g(\theta; \alpha)}{\beta_0}. \quad (15)$$

Given an end-test threshold $1/40$, the $LCI^{(m^*)}$ is therefore wholly defined as a function of the model parameters γ , α , and β_0 :

$$LCI^{(m^*)} = \frac{g(\min\{k : f(k; \gamma) \leq 1/40\}, \alpha)}{\beta_0}. \quad (16)$$

We fitted the models using a Bayesian approach, assigning either diffuse or informative prior distributions to the parameters as described in Table 1. Diffuse distributions contained only vague information based on the potential scale and theoretical support of a parameter [17]. These priors have the advantage over wider, less informative priors in that they aid computation and inference while providing only minimal information. We used half-Cauchy distributions as diffuse priors for the scale parameters, as previously recommended [17, 18]. Informative prior distributions, on the other hand, were intended to characterise the typical distribution of the MBW model parameters. The informative priors were obtained by fitting a two-level hierarchical model for GAS, CEVGM, and CEVTG to all of our data, as outlined in the Appendix.

We fitted the models with both diffuse and informative priors to each individual test with complete data and calculated the posterior medians of $CEV^{(m)}$, $FRC^{(m^*)}$, and $LCI^{(m^*)}$ in both cases, which we refer to herein as the 'model-based' estimates.

Assessing agreement and variance

We assessed agreement and compared the variances of the model-based and standard methods using a linear mixed-effects (LME) model. Since the MBW tests in our study were performed multiple times on the same participant, we needed a model flexible enough to account for replicate measurements. We use a variation of a model proposed by Carstensen et al. [19], which accounts for variation between participants and also variation due to replicate measurements. Whereas Carstensen et al. model the between-participant variation using fixed effects, in the Bayesian setting, and with a large number of participants, we found that these were more naturally modelled as random effects.

Denoting the method of measurement by m , where $m = 1$ denotes the standard method, $m = 2$ denotes the model-based method using diffuse priors, and $m = 3$ denotes the model-based method using informative priors, the study participants by p ($p = 1, \dots, 432$), and the r 'th replicate of method m on participant p as y_{mpr} , the model is defined as:

$$\begin{aligned}
y_{mpr} &= \alpha_m + u_p + a_{pr} + c_{mp} + e_{mpr}, \\
u_p &\sim N(0, \gamma), \quad a_{pr} \sim N(0, \omega), \quad c_{mp} \sim N(0, \tau_m), \quad e_{mpr} \sim N(0, \sigma_m), \\
\alpha_m &\sim N(0, 10^4), \quad \gamma, \omega, \tau_m, \sigma_m \sim \text{Half-Cauchy}(0, 2.5),
\end{aligned} \tag{17}$$

where α_m is the mean effect for method m , the variation between participants is captured by γ , the variation between replicates (nested within participants) is captured by ω , the variation between participants across replicates for each method is captured by τ_m , and the within-participant variation for a specific method m (i.e. across replicates) is captured by the residual σ_m . Note that the inclusion of the a_{pr} term makes this correspond to the 'linked replicates' model of Carstensen et al.

For simplicity, we assumed that $\tau_1 = \tau_2 = \tau_3 = \tau$; the size of this component was estimated to be negligible in our data, see Results. In our case, although the data used for each estimation method (for a given individual and replicate test) were identical, we assumed an exchangeable replicate structure, dropping the a_{pr} terms, so as not to overparameterise the model. This allowed us to estimate a separate residual variance for each method, albeit with the variation due to replicates, which would otherwise be captured by ω , being distributed among the estimable variance components γ , τ , and σ_m . However, it was also of interest to understand the size of the per-replicate variation, so we fitted a second model where we included a_{pr} but assumed a common residual variance for each method; i.e. $\sigma_1 = \sigma_2 = \sigma_3 = \sigma$.

We again took a Bayesian modelling approach and assigned diffuse priors on the model parameters [17, 18]: normal distributions for the mean components, and half-Cauchy distributions for the variance components, as shown in (17).

Assessing shortened tests

We assessed the accuracy of our model when using shortened test data. For each test, we truncated each of $c(k)$, $v(k)$, and $r(k)$ up to the first k where $c(k)$ fell below some threshold and remained there for two subsequent breaths, in the same way that the standard method is used to empirically determine the end-test breath. This method of truncation is similar to that used by other studies that have evaluated the use of 'shortened' MBW tests [9–11]. We used six different thresholds for the tracer gas quantity: 1/3, 1/4, 1/5, 1/10, 1/20, and 1/30. We fitted our models to the six shortened test datasets to estimate the model-based LCI using either diffuse or informative priors as shown in Table 1.

We assessed the accuracy of our model, for each of the six truncation thresholds, by examining the distribution of prediction errors and the width of the 95% credible intervals (CI) of the predictions, as a proportion of the model-based LCI estimates using the complete test data.

Model estimation

We took a Bayesian approach to estimating our model parameters for a number of reasons. First, the approach makes it relatively straightforward to define and estimate derived parameters such as the model-based LCI by sampling from the posterior distribution in Stan, a probabilistic programming language [20]. This allows us to quantify the uncertainty around our model-based LCI using Markov chain Monte Carlo (MCMC) methods. Second, the Bayesian approach allows us to naturally incorporate prior information in our model parameters. By assigning prior distributions to our model parameters we are able to constrain them to realistic values which can be effectively updated with the available data given different levels of test completion. The Stan model code and a description of the data used are provided in the Supplementary material.

We sampled from the posterior distribution of each parameter estimated in this paper using the Hamiltonian Monte Carlo (HMC) algorithm implemented within Stan, called from the R software

environment [21]. In each case, four MCMC chains were run in parallel comprising a discarded ‘warm-up’ phase and a ‘sampling’ phase, the latter being used for parameter estimation. The length of the parameter chains were run for 500 warm-up iterations followed by 500 sampling iterations resulting in 2,000 samples from the posterior distribution for each parameter.

Convergence of the Markov chains was assessed both graphically, via visual inspection of the MCMC chains, and statistically, by ensuring that the scale reduction factor \hat{R} was near 1 for each parameter [22]. The analysis of shortened tests was done for each of the six artificially shortened datasets from the 1,197 available MBW tests, and both diffuse and informative prior distributions, resulting in 14,364 separate analyses. Since it is impractical to assess the convergence of so many tests graphically, for these analyses convergence was assessed to be sufficient for a single test if all parameters had scale reduction factors (\hat{R}) below 1.25.

Results

Analysis of complete tests

The MBW models were fitted to each of the 1,197 available MBW tests. Parameter convergence was sufficient in most cases, with \hat{R} values close to 1. Although for a handful of tests a small number of parameters exhibited sub-optimal convergence, this was judged unlikely to materially affect the overall results. The model fit for a typical individual’s MBW data with informative prior information is shown in Figure 3, along with 10 simulated datasets drawn from the posterior predictive distribution for each quantity. The model appears to describe the data well on the transformed scale (left column), and on the original scale (right column). Although we show a single test in Figure 3, we observed similar results for a number of other tests. The fit of the CEVTG data on the original scale may at first glance appear unsatisfactory, but note that our model of the logged increments of CEVTG is a good fit to the transformed data and because CEVTG is a cumulative measure of a decreasing quantity, the observed CEVTG curves are heavily influenced by any noise in the early breaths of the washout. We therefore

reason that the posterior fit provides a good representation of the true underlying process and that the observed data on the cumulative scale are in fact a very noisy representation of this process.

Scatterplots of the LCI, CEV, and FRC estimated by each method are shown in Figure 4. The model-based method, using either diffuse or informative priors, produced FRC and CEV estimates that were, on average, slightly lower than the standard method estimates. However, the resulting estimates of LCI appeared to be similar nonetheless. In contrast to the diffuse priors, using informative priors seemed to shrink some of the more extreme FRC estimates down towards more representative and clinically realistic values.

The posterior medians and 95% CIs for the parameters of the LME model assuming exchangeable replicates and method-specific residuals are summarised in Table 2. Parameter convergence was sufficient in all cases. The differences between the mean components of the standard and model-based methods for LCI were relatively small with $\alpha_1 - \alpha_2$ at 0.03 (95% CI: 0.00, 0.05) and $\alpha_1 - \alpha_3$ at -0.01 (95% CI: -0.03, 0.02). On average, the model-based method provided smaller estimates for CEV, with $\alpha_1 - \alpha_2$ at 23.80 mL (95% CI: 20.02, 27.64) and $\alpha_1 - \alpha_3$ at 23.37 mL (95% CI: 19.38, 27.26). This was presumably due to the use of the model-based end-test definition which, by nature, is typically earlier than when using the standard method. Model-based FRC estimates were on average smaller as well, with $\alpha_1 - \alpha_2$ at 3.2 mL (95% CI: 2.51, 3.89) and $\alpha_1 - \alpha_3$ at 4.10 mL (95% CI: 3.42, 4.86). This seemed to be due to the model controlling for noisy measurements at the start of the test, which tended to have an upward influence on subsequent observations. These differences between the methods appeared to roughly cancel out when taking their ratio to calculate LCI.

The residual variance component of the model-based LCI obtained using diffuse priors was slightly higher than under the standard method (σ_1/σ_2 estimated at 0.91; 95% CI: 0.85, 0.96), but very similar when using informative priors (σ_1/σ_3 0.98; 95% CI: 0.92, 1.04). However, these difference are quite minor when compared to the overall magnitude of variation. The pattern

was similar for the residual variance components of FRC, with σ_1/σ_2 at 1.00 (95% CI: 0.92, 1.02) and σ_1/σ_3 at 1.10 (95% CI: 1.01–1.13). On the other hand, the residual variances of the model-based methods for CEV were lower than for the standard method, with σ_1/σ_2 at 1.09 (95% CI: 1.03, 1.16) and σ_1/σ_3 at 1.11 (95% CI: 1.05, 1.17), which may be explained by the definitions of stopping time (see previous). The method-participant interaction parameter, τ , was relatively small for each outcome which was not surprising, considering we are comparing similar methods. Interestingly, for CEV and FRC the within-participant (residual) variation for each method was about half the size of the between-participant variation (γ), but for LCI these were roughly similar to each other.

The posterior medians and 95% CIs for the parameters of the LME model assuming non-exchangeable replicates and a single common residual term are summarised in Table 3. The main purpose of fitting this model was to investigate the extent that the exchangeable model assumption affected our interpretation of the variation and residual components of the model. As the table shows, the mean components remained similar, but a substantial amount of variation was ‘redirected’ to the replicate-participant interaction term ω from the between-participant interaction γ and the residual σ . This suggested that a substantial amount of the residual variation in Table 2 is in fact due to the variation between replicates.

Note that the purpose of this analysis was not to strictly establish equivalence or interchangeability between the two measurement systems, but rather to examine how they differed, and whether we were satisfied that the differences are justified. When using informative prior information, the mean and residual components of the main parameter of interest, LCI, were similar. Likewise, although the mean components of the model-based CEV and FRC were lower than the standard method, this is expected given the models used to estimate these quantities. Furthermore, the residual components of CEV and FRC were lower when using informative priors, although this is likely due to the fact that the model-based estimates of these parameters are positive and smaller in magnitude. This suggests that our

informative prior model produces estimates of LCI that could be used interchangeably with the standard method.

Analysis of shortened tests

We fitted the MBW models to the six artificially shortened MBW tests corresponding to the 1,197 complete MBW tests. In general, as shown in Table 4, relatively few tests exhibited sub-optimal MCMC convergence. In any case, using stronger prior information appeared to solve most convergence issues, and in the cases where convergence was not sufficient, it is likely that finer tuning of the MCMC sampler or additional sampling iterations would have resolved the issue. Regardless, dropping the estimates from tests that had convergence issues had negligible impact on these results for both the diffuse and informative prior information cases, and thus we did not remove them from the results shown here.

Figure 5 shows plots of the median and the 2.5th and 97.5th percentiles of the prediction errors and the width of the 95% credible intervals, for each of the shortened datasets across all 1,197 MBW tests, as a percentage difference of the known model-based LCI estimate using complete data and either diffuse or informative priors. Figure 6 shows similar information to Figure 5, but for estimates of FRC rather than LCI.

For LCI, in both diffuse and informative prior information cases, the accuracy of the model-based estimate clearly improved with more data. Furthermore, in each shortened test scenario, the median prediction error was less than 10% in both diffuse and informative prior information cases. This indicates that the model estimates are generally accurate even when the data are highly incomplete. The informative priors helped to moderate the estimates, particularly when the tests were highly incomplete, reducing the bias that was discernible with the diffuse priors. The range of the prediction errors shrank as we considered longer tests, showing how the estimates become progressively more reliable. For shortened test thresholds

higher than 1/10, the model was clearly more reliable when using informative priors, but the difference between the priors was relatively small for thresholds of 1/10 or lower.

As shown in Figure 6, the results were similar for estimation of FRC, although the model-based FRC showed no discernible bias in either the diffuse and informative prior cases, and the range of the prediction errors was smaller than that of LCI for both cases, with the exception of tests shortened to tracer gas quantities higher than 1/10 in the diffuse case.

The downward bias of LCI for very short tests when using diffuse priors can be understood in the context of the underlying log discrete derivative models used for CEVGM and CEVTG, which are linear, and thus can be extrapolated with some accuracy beyond their range. On the other hand, the underlying model for θ_i is a mixture of fast and slow decaying exponential components. With only a limited amount of data (due to short tests) and absence of informative priors to constrain the two components, the model placed a greater weight on the fast decaying component, which dominates in the earlier stages of the test, resulting in a smaller θ_i , and thus smaller $CEV^{(m)}$ and $LCI^{(m^*)}$. This was somewhat rectified by using informative priors, which ensured that the model properly acknowledged the existence of a slowly emptying compartment even when there were insufficient data to easily estimate it, resulting in a more accurate estimate of θ_i , and correspondingly better estimates of $CEV^{(m)}$ and $LCI^{(m^*)}$.

A clear issue with both the LCI and FRC estimates using shortened tests was the degree of uncertainty around each estimate. This is assessed in both Figure 5 and Figure 6 by summarising the proportional width of the 95% CI across the 1,197 estimates for each shortened test scenario. Uncertainty around estimates of both $FRC^{(m^*)}$ and $LCI^{(m^*)}$ using data shortened to thresholds higher than 1/10 is high enough to discourage any use of estimates from tests shorter than this level. However, the uncertainty appeared to stabilise at a level similar to the complete data case at thresholds equal to or lower than 1/10, particularly when using informative prior information. The fact that the uncertainty did not reduce beyond this threshold is likely representative of the inherent uncertainty in the underlying LCI definition.

Moreover, this suggests that there is little to be gained by performing the test for any longer than up to a tracer gas quantity threshold of around 1/10.

Discussion

As far as we know we are the first to use statistical models to define and then estimate the key parameters of the MBW, in particular LCI and FRC. By modelling the MBW data rather than using simple summaries, we developed a principled way of assessing the uncertainty in LCI estimates. Additionally, we applied these models to assess how much test data are required to obtain reasonable estimates of LCI and how the uncertainty around these estimates changes given different degrees of test completion.

Applying our model to complete MBW tests, we observed posterior predictive distributions that reflected the underlying structure and variation in the observed data. As part of this modelling process we also examined the variation structure of the MBW parameters in depth using a linear mixed-effects model. Our complete-data model-based estimates of LCI have good agreement and similar residual variance compared to the same quantities estimated using the standard empirical method. Moreover, using informative priors seems to constrain the estimation procedure to produce more realistic values of FRC when faced with extreme cases.

Our most important finding is that we were able to obtain reasonable estimates of LCI and FRC even with data shortened to a tracer gas quantity threshold as high as 1/10. On average, a complete test is 30 breaths in length, and a test shortened to the 1/10 tracer gas level is approximately 17 breaths, translating to an average 43% reduction in breaths required. For tests shortened to thresholds higher than this, our estimates became inaccurate. This suggests some portion of the test beyond the start but before the 1/10 threshold contains information necessary to determine LCI at the end of the test. This makes intuitive sense: because the areas of the lung with least ventilation are likely to take longer to empty, the slope of the tracer gas quantity curve is flatter later in the test. Predictions made without any data from this part of the

test will typically be underestimates because θ will typically be underestimated. From our results, it appears that, in general, sufficient additional information to reliably estimate LCI becomes available between proportions 1/5 and 1/10 (on average this gap spans approximately five breaths). Using our model it is unlikely that LCI can be reliably estimated from tests shorter than the 1/10 threshold tracer gas quantity.

Our exposition of a model-based LCI predicted from shortened tests indirectly supports recent studies that have found that an LCI defined using a higher tracer gas quantity threshold can still be clinically meaningful, e.g. $k^{(20)}$ and in some cases $k^{(10)}$, instead of $k^{(40)}$ [9–11]. However, we do not yet have MBW data from participants with known lung disease and thus cannot make a direct comparison.

Our model can produce reliable estimates of LCI from MBW tests that are, on average, 43% shorter than a complete test (measured by number of breaths). This potentially allows data that would otherwise be unused, due to artefacts or test disruption, to be shortened and subsequently analysed to estimate key quantities of lung function with good accuracy. Given the logistical challenges of conducting MBW testing in unsedated infants during natural sleep, this is an important finding as it may allow the various birth cohort studies that have undertaken MBW testing to utilise a larger proportion of their MBW data. At a clinical level, this new approach may save both patient and clinician time and effort as potentially fewer tests will be required to achieve the desired number of acceptable LCI measurements. At a broader level, incomplete MBW tests collected as part of large cohort studies may now become usable, increasing the amount of analysable data from such studies.

For this analysis, we have chosen not to model the tests jointly, but rather analyse each test separately. This is to reflect how MBW testing would be done in a clinical situation, with individual tests being performed and analysed sequentially, rather than together as a large cohort. This is also why we have chosen to approximate informative priors, which we used to estimate LCI with shortened data, based on hyperparameters of a comparatively simple two-

level hierarchical model (see Appendix). When asking epidemiological questions, there may be value for large cohorts such as this to implement our MBW models using a three-level hierarchy to share information between tests in a more rigorous, completely model-based fashion.

We have likewise chosen to model each of the functions $v(k)$, $r(k)$, and $c(k)$ independently for each MBW test. Although each quantity is undoubtedly related to the other—for example, the quantity of tracer gas expired is a product of the per-breath amount of total gases expired and the concentration of tracer gas within that breath—we have chosen not to define an explicit correlation structure for both simpler exposition and computation.

Additionally, when analysing the residual variances of each method we have made the assumption in our LME model of an exchangeable replicate structure. While it would have been useful to parse out the variation into individual components to the fullest extent possible by including an additional interaction term to account for the non-exchangeability of our replicates, we found that with this dataset it was not possible to do so while still being able to estimate the separate residual components for each method. Therefore the residual components of the LME model must be interpreted as containing some variation due to replicates within each participant.

The analyses reported here were limited to a population-derived infant sample. It is not clear how our model would perform with MBW data from a selected sample of participants with lung disease, but it is likely that for these participants there will be an even more pronounced change in the slope in the later part of the tracer gas quantity curve which could potentially make extrapolation into this area of the test less accurate using only shortened test data with diffuse prior information. A clear direction for future research is therefore to assess these models using MBW tests from both healthy and disease-affected infants.

Acknowledgments

The authors are grateful to the BIS study participants and their families for their contribution, and to Louise King and Hilianty Tardjono for their assistance in obtaining and processing the MBW data. We also thank the BIS investigator team for their collaboration in making this work possible.

This work was supported by the National Health and Medical Research Council: Centre of Research Excellence Grant ID 1035261 (Victorian Centre for Biostatistics; ViCBiostat), Senior Research Fellowship ID 1110200 (Anne-Louise Ponsonby), and Project Grant ID 1009044. Robert Mahar was supported by the Australian Government Research Training Program Scholarship. The MBW testing equipment was purchased by the Shane O'Brien Memorial Asthma Foundation. Research at the Murdoch Childrens Research Institute is supported by the Victorian Government's Operational Infrastructure Support Program.

References

1. Morgan WJ, Stem DA, Sherrill DL, et al (2005) Outcome of asthma and wheezing in the first 6 years of life: follow-up through adolescence. *Am J Respir Crit Care Med* 172:1253–1258.
2. Hülskamp G, Pillow JJ, Stocks J (2005) Lung function testing in acute neonatal respiratory disorders and chronic lung disease of infancy: a review series. *Pediatr Pulmonol* 40:467–470. doi: 10.1002/ppul.20317
3. Beydon N, Davis SD, Lombardi E, et al (2007) Pulmonary function testing in preschool children. *Am J Respir Crit Care Med* 175:1304–1345. doi: 10.1164/rccm.200605-642ST
4. Saline Hypertonic in Preschoolers with Cystic Fibrosis and lung structure as measured by computed tomography (CT). SHIP-CT study.
5. Robinson PD, Latzin P, Verbanck S, et al (2013) Consensus statement for inert gas washout measurement using multiple- and single- breath tests. *Eur Respir J* 41:507–522. doi: 10.1183/09031936.00069712
6. Rosenfeld M, Allen J, Arets BHGM, et al (2013) An Official American Thoracic Society Workshop Report: Optimal Lung Function Tests for Monitoring Cystic Fibrosis, Bronchopulmonary Dysplasia, and Recurrent Wheezing in Children Less Than 6 Years of Age. *Ann Am Thorac Soc* 10:S1–S11. doi: 10.1513/AnnalsATS.201301-017ST
7. Horsley A (2009) Lung clearance index in the assessment of airways disease. *Respir Med* 103:793–799. doi: 10.1016/j.rmed.2009.01.025
8. Vukcevic D, Carlin JB, King L, et al (2015) The influence of sighing respirations on infant lung function measured using multiple breath washout gas mixing techniques. *Physiol Rep* 3:e12347–e12347. doi: 10.1481/phy2.12347
9. Singer F, Yammie S, Abbas C, et al (2012) Ways to shorten the lung clearance index measurement II-How long to wash? *Eur Respir J* 40:3298.
10. Yammie S, Singer F, Abbas C, et al (2013) Multiple-breath washout measurements can be significantly shortened in children. *Thorax* 68:586–587. doi: 10.1136/thoraxjnl-2012-202345
11. Hannon D, Bradley JM, Bradbury I, et al (2014) Shortened lung clearance index is a repeatable and sensitive test in children and adults with cystic fibrosis. *BMJ Open Respir Res* 1:e000031.
12. Vuillermin P, Saffery R, Allen KJ, et al (2015) Cohort Profile: The Barwon Infant Study. *Int J Epidemiol* 44:1148–1160. doi: 10.1093/ije/dyv026
13. Bennett J (2015) AutoIt. AutoIt Consulting
14. Schibler A, Henning R (2001) Measurement of functional residual capacity in rabbits and children using an ultrasonic flow meter. *Pediatr Res* 49:581–588.
15. Bates JHT (2009) Lung mechanics: an inverse modeling approach. Cambridge University Press, Leiden
16. Gonem S, Scadding A, Soares M, et al (2014) Lung clearance index in adults with non-cystic fibrosis bronchiectasis. *Respir Res* 15:59.

17. Stan Development Team (2016) Stan Modeling Language: User's Guide and Reference Manual. Version 2.12.0.
18. Gelman A, others (2006) Prior distributions for variance parameters in hierarchical models. *Bayesian Anal* 1:515–534.
19. Carstensen B, Simpson J, Gurrin LC (2008) Statistical models for assessing agreement in method comparison studies with replicate measurements. *Int. J. Biostat.* 4:
20. Stan Development Team (2016) The Stan C++ Library.
21. Stan Development Team (2016) RStan: the R interface to Stan.
22. Gelman A, Carlin C John B, Stern HS, et al (2013) Bayesian Data Analysis, Third. CRC Press

Appendix

The parameters of the informative prior distributions used in this paper, shown in Table 1, were obtained using a two-level hierarchical model for GAS, CEVGM, and CEVTG, as described by equations (18), (19), and (20). The lower level of this model was the same as the model described in the Methods that we fitted to each individual test, while the upper level allowed us to characterise the overall variation of each of the parameters. We fitted this two-level model to all 1,197 tests with complete data. The posterior medians of the hyperparameters were extracted for use as parameters of the informative prior distributions.

Thus we modelled the log of the tracer gas quantity c_i hierarchically as:

$$\begin{aligned}
 c_i(k) &\sim LN(f(k; \gamma_i), \sigma_{ci}) \\
 \gamma_{0i} &\sim N(\mu_{\gamma_0}, \sigma_{\gamma_0}), \quad \gamma_{1i} \sim N(\mu_{\gamma_1}, \sigma_{\gamma_{1i}}), \quad \gamma_{2i} \sim N(\mu_{\gamma_1}, \sigma_{\gamma_{1i}}), \quad \mu_{\gamma_0} \sim \text{Beta}(2, 2), \\
 \mu_{\gamma_1}, \mu_{\gamma_2} &\sim N(0, 10), \quad \sigma_{ci} \sim N(\mu_{\sigma_c}, \varepsilon_c), \quad \sigma_{\gamma_0}, \sigma_{\gamma_1}, \sigma_{\gamma_2}, \mu_{\sigma_c}, \varepsilon_c \sim \text{Half-Cauchy}(0, 2.5).
 \end{aligned} \tag{18}$$

Likewise the log of the discrete derivative of v_i was modelled as:

$$\begin{aligned}
 v'_i(k) &\sim LN(g'(k; \alpha_i), \sigma_{vi}) \\
 \alpha_i &\sim N(\mu_\alpha, \sigma_\alpha), \quad \sigma_{vi} \sim N(\mu_{\sigma_v}, \varepsilon_v), \quad \mu_\alpha \sim N(0, 10^2), \quad \sigma_\alpha, \mu_{\sigma_v}, \varepsilon_v \sim \text{Half-Cauchy}(0, 2.5),
 \end{aligned} \tag{19}$$

And the log of the discrete derivative of r_i was modelled as:

$$\begin{aligned}
 r'_i(k) &\sim LN(h'_i(k; \beta_i), \sigma_{ri}) \\
 \beta_{0i} &\sim N(\mu_{\beta_0}, \sigma_{\beta_0}), \quad \beta_{1i} \sim N(\mu_{\beta_{1i}}, \sigma_{\beta_{1i}}), \quad \mu_{\beta_0} \sim N(0, 10^3), \quad \mu_{\beta_1} \sim N(0, 10), \\
 \sigma_{ri} &\sim N(\mu_{\sigma_r}, \varepsilon_r), \quad \sigma_{\beta_0}, \sigma_{\beta_1}, \mu_{\sigma_r}, \varepsilon_r \sim \text{Half-Cauchy}(0, 2.5).
 \end{aligned} \tag{20}$$

These models are similar to their non-hierarchical counterparts, but allow the sharing of information between tests by modelling the lower-level parameters as coming from a common distribution. As recommended, diffuse priors were used on the mean parameters and half-Cauchy priors for the scale parameters [18].

To determine whether we are justified in using prior distributions approximated from the same data, we confirmed the stability of our posterior hyperparameters by fitting the same two-level model to three training datasets containing a randomly selected subset, without replacement, of 399 participants. Doing this allowed us to confirm that the posterior distributions of our hyperparameters were relatively stable across subsets (data not shown). As our primary interest here was to approximate our model parameter's prior distributions for use with future tests, we deliberately used the simpler two-level hierarchical model rather than a more complex three-level model that would account for the fact that we had multiple replicates for each participant.

Tables

Table 1

Prior distributions. The prior distributions for the model parameters used to model individual tests. Each of the distributions stated below are truncated to the support of each respective parameter.

Parameter	Diffuse prior	Informative prior
γ_0	Beta(2, 2)	N(0.63, 0.18)
γ_1	N(0, 10)	logN(0.12, 0.17)
γ_2	N(0, 10)	logN(0.4, 0.47)
α	N(0, 100)	N(30, 6.5)
β_0	N(0, 1000)	N(126, 18)
β_1	N(0, 10)	N(0.136, 0.024)
σ_c	Half-Cauchy(0, 2.5)	N(0.06, 0.02)
σ_r	Half-Cauchy(0, 2.5)	N(0.2, 0.047)
σ_v	Half-Cauchy(0, 2.5)	N(0.09, 0.026)

Table 2

Agreement analysis: exchangeable replicates, method-specific residuals. Parameter estimates (posterior medians and 95% credible intervals) from the LME model fitted to the BIS MBW outcomes, comparing standard and model-based estimates.

Parameter	LCI		CEV (mL)		FRC (mL)	
	Median	95% CI	Median	95% CI	Median	95% CI
Mean components						
Standard method (α_1)	6.10	(6.07, 6.14)	796.66	(783.43, 807.1)	130.90	(128.91, 133.24)
Model-based method: diffuse (α_2)	6.08	(6.04, 6.12)	773.07	(759.2, 783.35)	127.70	(125.75, 129.94)
Model-based method: informative (α_3)	6.11	(6.07, 6.15)	773.44	(759.33, 783.55)	126.80	(124.82, 129.06)
<i>Mean difference</i> ($\alpha_1 - \alpha_2$)	0.03	(0, 0.05)	23.80	(20.02, 27.64)	3.20	(2.51, 3.89)
<i>Mean difference</i> ($\alpha_1 - \alpha_3$)	-0.01	(-0.03, 0.02)	23.37	(19.38, 27.26)	4.10	(3.42, 4.86)
Variation components						
Between-participant (γ)	0.32	(0.3, 0.35)	112.25	(104.57, 119.93)	19.30	(18.08, 20.62)
Method-participant interaction (τ)	0.01	(0, 0.02)	0.64	(0.04, 2.02)	0.10	(0.01, 0.45)
Residual components						
Standard method (σ_1)	0.34	(0.33, 0.36)	51.16	(49.14, 53.32)	8.60	(8.24, 8.94)
Model-based method: diffuse (σ_2)	0.38	(0.36, 0.39)	46.76	(44.96, 48.67)	8.90	(8.51, 9.23)
Model-based method: informative (σ_3)	0.35	(0.33, 0.36)	46.20	(44.42, 48.05)	8.00	(7.69, 8.37)
<i>Residual ratio</i> (σ_1/σ_2)	0.91	(0.85, 0.96)	1.09	(1.03, 1.16)	1.00	(0.92, 1.02)
<i>Residual ratio</i> (σ_1/σ_3)	0.98	(0.92, 1.04)	1.11	(1.05, 1.17)	1.10	(1.01, 1.13)

Notes: LCI: lung clearance index; CEV: cumulative expired volume; FRC: functional residual capacity; CI: credible interval.

Table 3

Agreement analysis: non-exchangeable replicates, common residuals. Parameter estimates (posterior medians and 95% credible intervals) from the LME model fitted to the BIS MBW outcomes, comparing standard and model-based estimates.

Parameter	LCI		CEV (mL)		FRC (mL)	
	Median	95% CI	Median	95% CI	Median	95% CI
Mean components						
Standard method (α_1)	6.10	(6.07, 6.14)	795.89	(785.84, 806.73)	131.00	(129.12, 132.8)
Model-based method: diffuse (α_2)	6.07	(6.04, 6.11)	771.96	(761.96, 782.74)	127.80	(125.93, 129.6)
Model-based method: informative (α_3)	6.11	(6.07, 6.14)	772.37	(762.39, 783.24)	126.60	(124.77, 128.48)
<i>Mean difference</i> ($\alpha_1 - \alpha_2$)	0.03	(0.02, 0.04)	23.94	(22.73, 25.07)	3.20	(2.83, 3.55)
<i>Mean difference</i> ($\alpha_1 - \alpha_3$)	-0.01	(-0.02, 0.01)	23.58	(22.45, 24.64)	4.40	(4.01, 4.69)
Variation components						
Between-participant (γ)	0.24	(0.21, 0.27)	103.72	(96.68, 112.71)	18.00	(16.55, 19.41)
Replicate-participant interaction (ω)	0.39	(0.37, 0.41)	54.86	(52.11, 57.58)	9.60	(9.11, 10.08)
Method-participant interaction (τ)	0.06	(0.05, 0.07)	3.74	(2.63, 4.67)	2.40	(2.27, 2.6)
Common residuals (σ)	0.12	(0.12, 0.12)	12.50	(12.08, 12.94)	1.90	(1.78, 1.92)

Notes: LCI: lung clearance index; CEV: cumulative expired volume; FRC: functional residual capacity; CI: credible interval.

Table 4

Summary of MCMC convergence for the analysis of shortened tests. The proportion of tests that exhibited sub-optimal parameter convergence, by having $\hat{R} > 1.25$ for at least one test parameter, in the shortened tests analysis

Shortened test length	Proportion of tests with convergence issues (%)	
	Diffuse prior	Informative prior
1/3	21%	5%
1/4	13%	3%
1/5	11%	2%
1/10	7%	0%
1/20	4%	<1%
1/30	3%	1%
Complete data	3%	<1%

Figures

Figure 1

Example of raw MBW data. Air flow (L/s) and molar mass (g/mol), shown over time (s) for a representative test. The left panels show the data for both the wash-in and washout phases; the right panels show the data for the washout phase only.

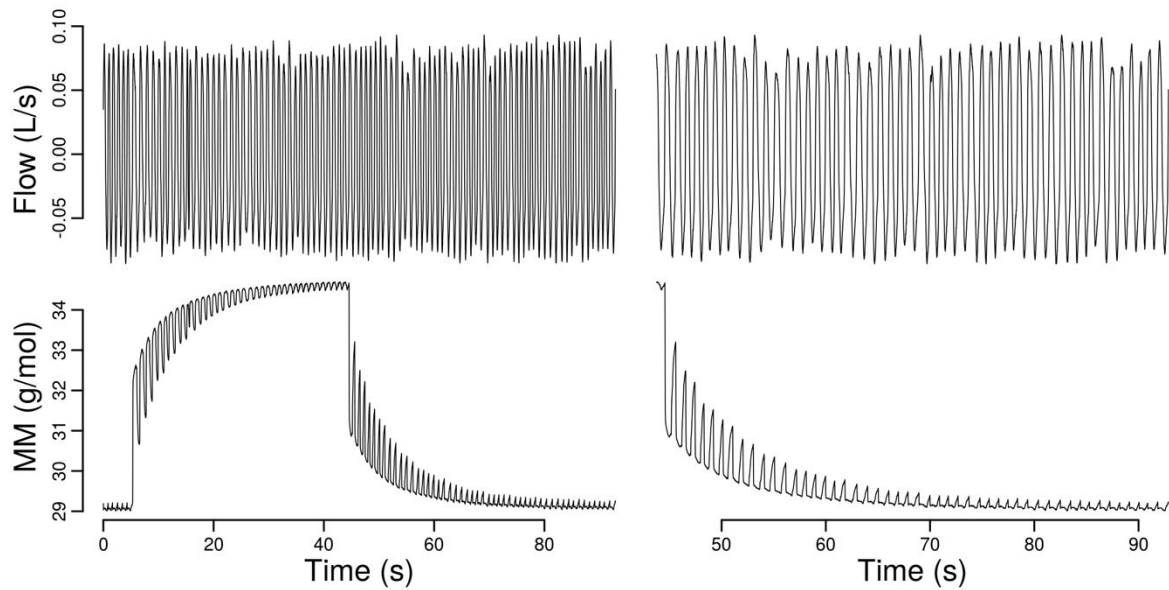


Figure 2

Example of derived MBW test quantities. These are shown for 10 randomly selected tests. GAS: tracer gas quantity (%); CEVGM: cumulative expired volume of gas mixture (mL); CEVTG: cumulative expired volume of tracer gas (mL).

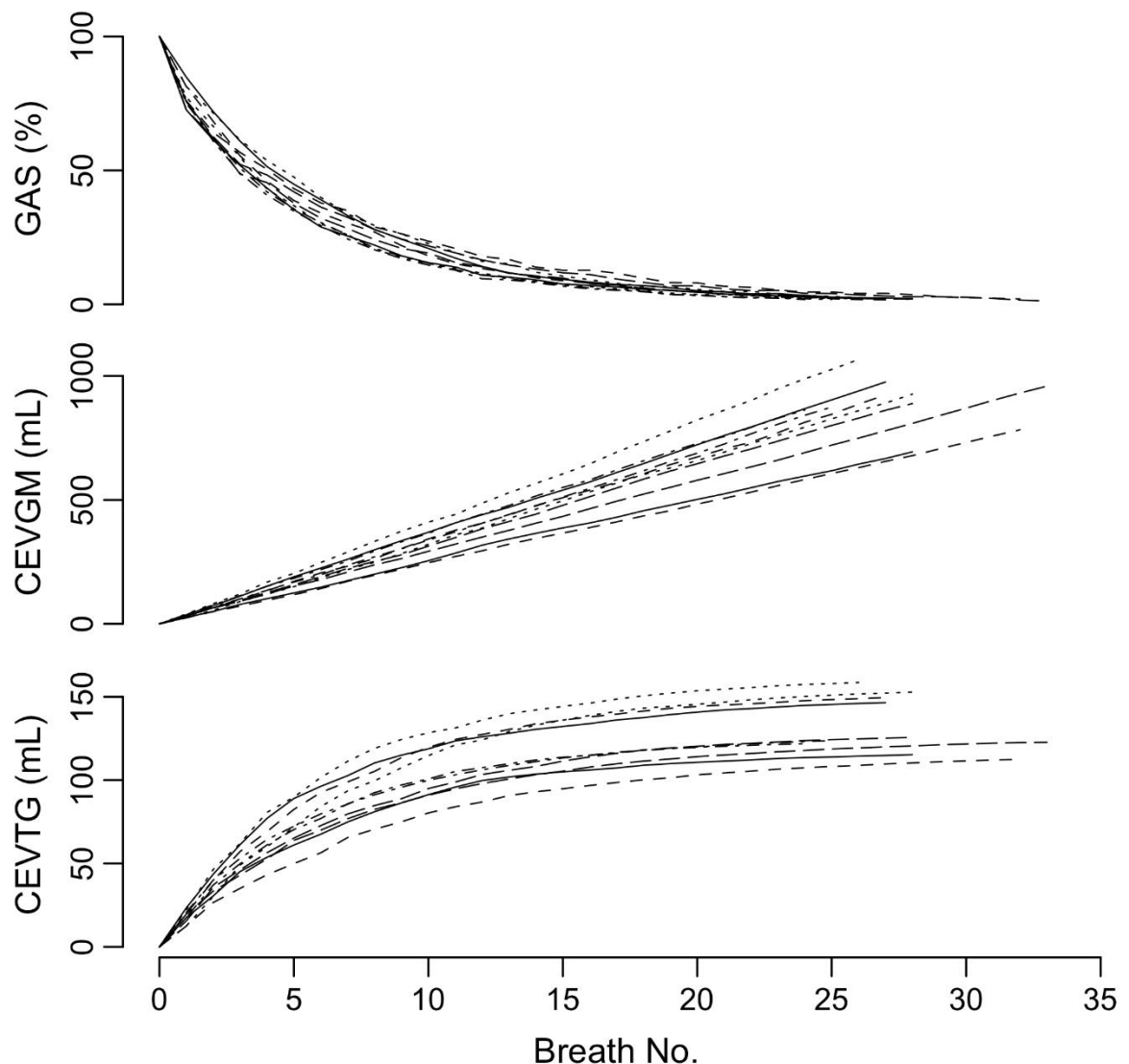


Figure 3

Example of a model fit. Plots showing, for a typical test and informative priors, the observed data (points), model-based mean prediction (black line), and a sample of posterior predictive draws (grey lines). The panels in the left column show the quantities on the transformed scale, while those in the right column show them on the original scale.

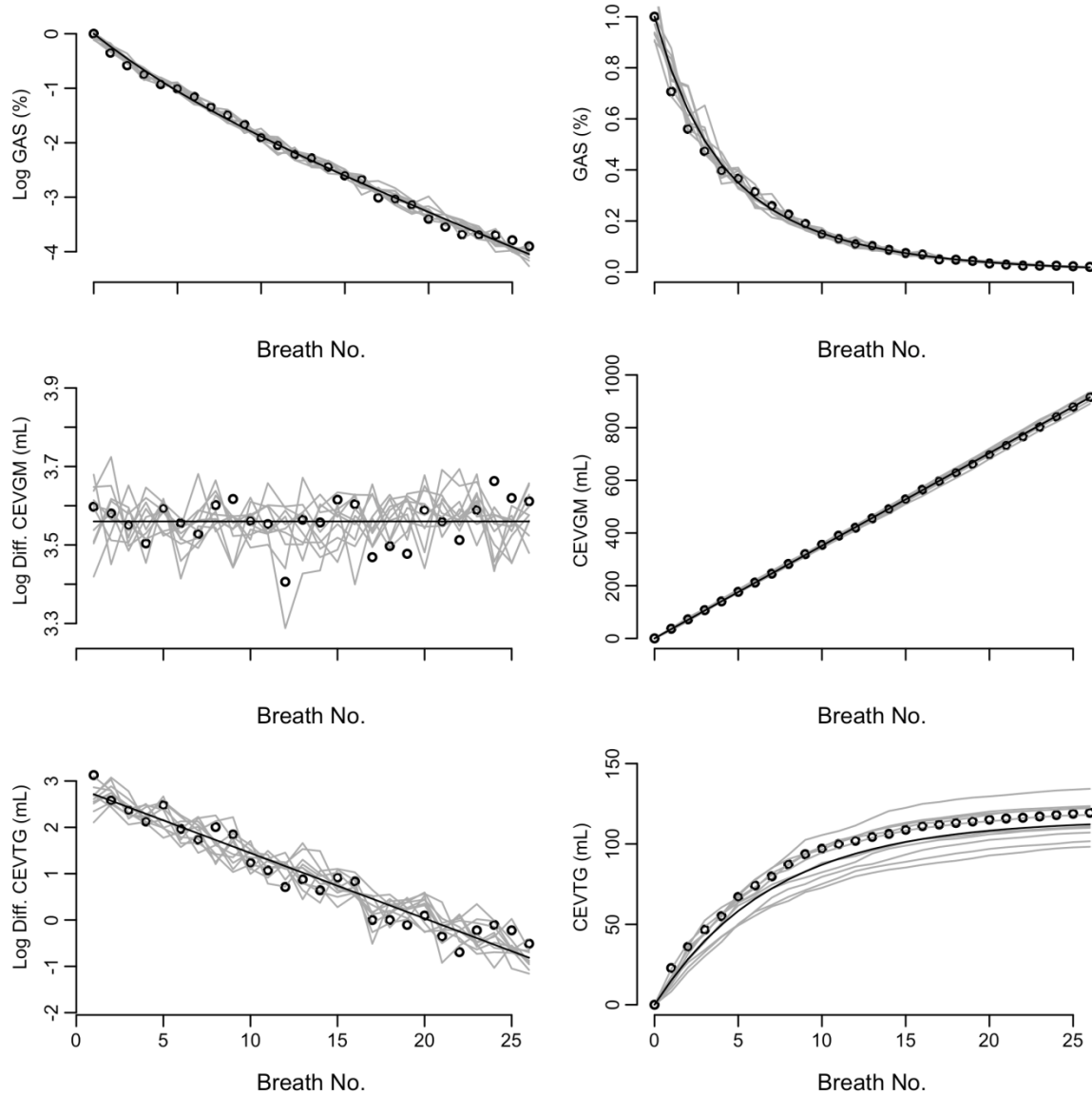


Figure 4

Comparison of estimation methods. Scatterplots showing comparison of MBW quantities estimated with complete data using either the standard or model-based methods (the latter with either the diffuse or informative priors) ($n = 1,197$). LCI: lung clearance index; CEV: cumulative expired volume (mL); FRC: functional residual capacity (mL).

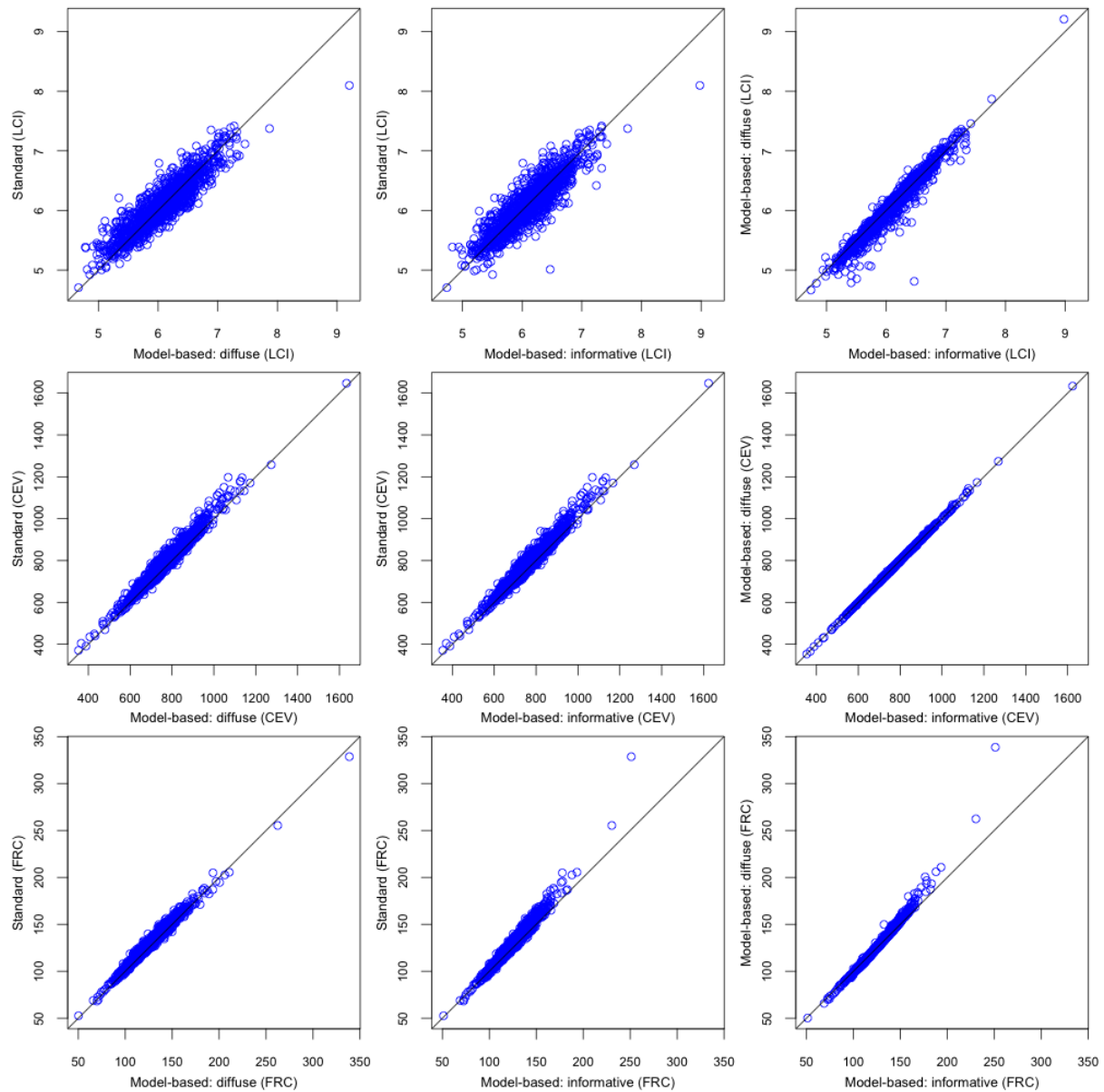


Figure 5

Estimation performance of LCI using shortened tests. The distributions of the prediction errors and 95% credible interval widths of the model-based LCI estimates (as a proportion of estimates using complete test data) based different degrees of test completeness and either diffuse or informative prior information ($n = 1,197$). Solid blue lines: median of pooled estimates; dashed blue lines: 2.5th and 97.5th percentiles of pooled estimates; shortened test lengths correspond to a tracer gas quantity; 'All': refers to estimates from tests using complete data, included for reference.

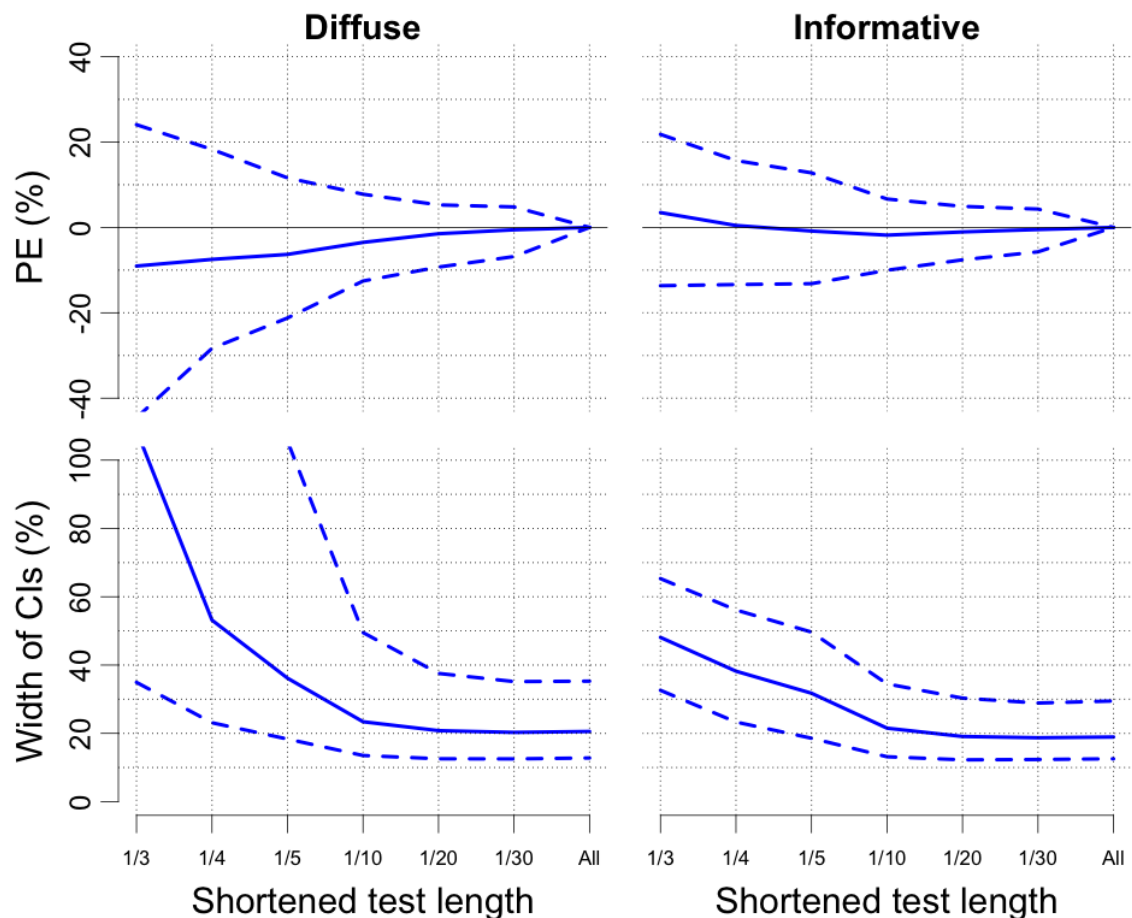
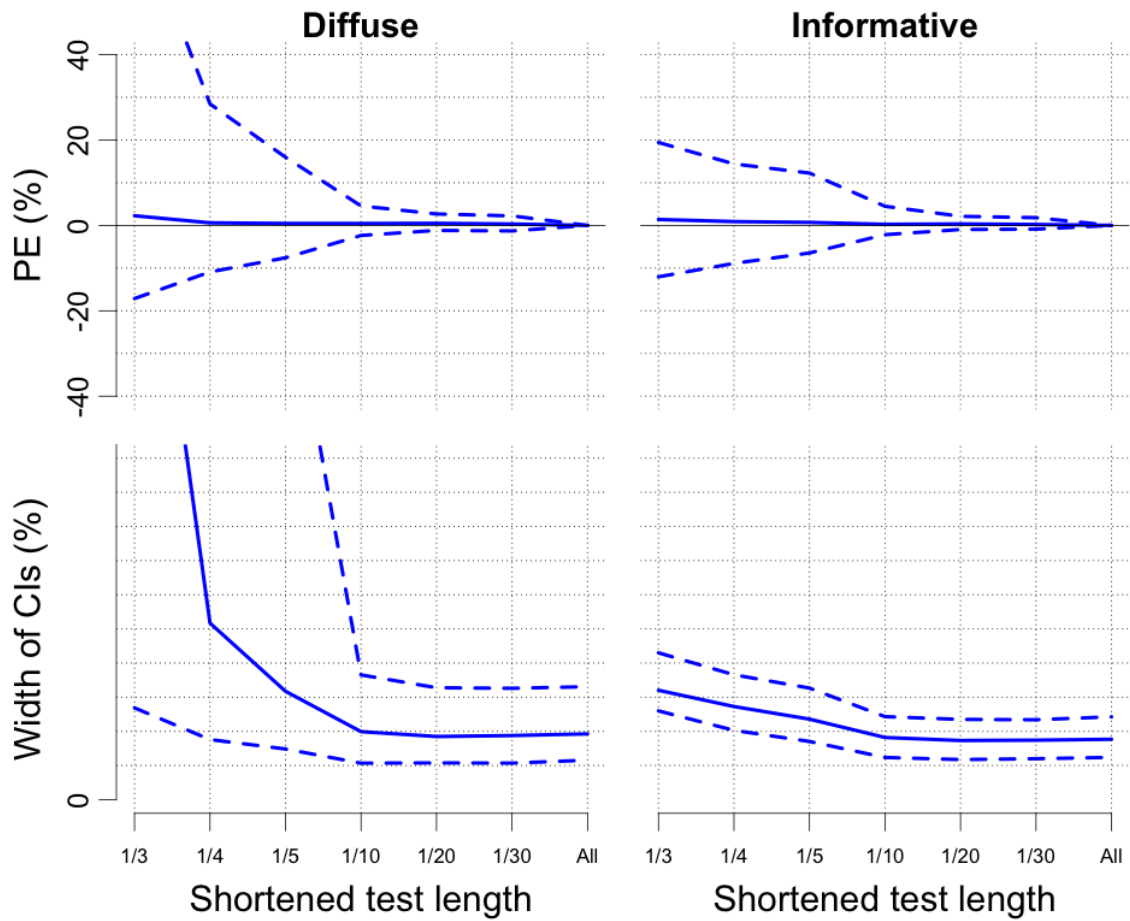


Figure 6

Estimation performance of FRC using shortened tests. The same as Figure 5 but now for estimates of FRC rather than LCI.



Supplementary material for “Bayesian modelling of repeated measures lung function data from multiple-breath washout tests”

We include Stan code for four models included in the main manuscript:

- Individual MBW models
 - o Using the diffuse prior (`mbw_individual_diffuse.stan`)
 - o Using the informative prior (`mbw_individual_informative.stan`)
- Linear mixed-effects (LME) models:
 - o Exchangeable replicates and method-specific residuals (`lme_exchangeable_separate.stan`)
 - o Linked replicates and common residuals (`lme_linked_common.stan`)

These models require the use of Stan through one of its interfaces, e.g. RStan, PyStan, CmdStan. We used RStan (version 2.12.1) implemented in R (version 3.3.1). More information is available at <http://mc-stan.org/>.

Data for the individual MBW models (`mbw_individual_diffuse.stan`, `mbw_individual_informative.stan`) should be a list containing the following objects:

- `M`: an integer count of the number of washout breaths measured in this test,
e.g. `int 30`
- `k`: an integer-valued vector containing the index number of each breath (counting from the start of the washout),
e.g. `num [1:30] 0 1 2 3 4 5 6 7 8 9 ...`
- `gas`: a real-valued vector containing the tracer gas quantity (GAS) at the end of the breath indexed by `k`,
e.g. `num [1:30] 1 0.701 0.501 0.404 0.390 ...`
- `cevgm`: a real-valued vector containing the observed cumulative expired volume of gas mixture (CEVGM) at the end of the breath indexed by `k`,
e.g. `num [1:30] 0 36.2 72.0 107.0 141.4 ...`
- `cetgv`: a real-valued vector containing the observed cumulative expired volume of tracer gas (CETGV) at the end of the breath indexed by `k`,
e.g. `num [1:30] 0 22.1 36.4 46.9 55.0 ...`

Supplementary material

Data for the LME models (`lme_exchangeable_separate.stan`, `lme_linked_common.stan`) should be a list containing the following objects (note that the LME model using exchangeable replicates does not require the vector `repl_ind`):

- `n_item`: an integer count of the number of items (participants) in the analysis,
e.g. `int 10`
- `n_all`: an integer count of the total amount of observations,
e.g. `int 100`
- `n_meth`: an integer count of the total number of methods to be compared,
e.g. `int 3`
- `y`: a real-valued vector containing the observations to compare,
e.g. `num [1:100] 111.1 100.1 120.2 110.8 180.9 ...`
- `item`: an integer-valued vector specifying the item (participant) index for each observation,
e.g. `int [1:100] 1 1 1 1 1 1 2 2 2 2 ...`
- `meth`: an integer-valued vector specifying the method index for each observation,
e.g. `int [1:100] 1 1 1 1 1 1 1 1 1 1 ...`
- `repl_ind`: an integer-valued vector specifying the replicate index for each observation (i.e. a separate index for each actual test conducted),
e.g. `int [1:100] 1 2 3 4 5 6 7 8 9 10 ...`

mbw_individual_diffuse.stan

```

functions {
  /**
   * Evaluate the tracer gas quantity at a particular time point.
   * This is a two-component exponential decay model.
   *
   * @param t      Time point at which to evaluate the gas quantity
   * @param lambda Mixture weight parameter (a.k.a. gamma0)
   * @param gamma  Exponents for each component
   *
   * @return Gas quantity (between 0 and 1) at the given time point.
   */
  real gas_curve(real t, real lambda, vector gamma) {
    return lambda * exp(-gamma[1] * t) + (1 - lambda) * exp(-gamma[2] * t);
  }

  /**
   * Determine if the tracer gas quantity crosses a given threshold between
   * two time points, t1 and t2.
   *
   * @param t1      First time point (left end of desired time interval)
   * @param t2      Second time point (right end of desired time interval)
   * @param threshold Threshold for the gas quantity
   * @param lambda  Mixture weight parameter (a.k.a. gamma0)
   * @param gamma   Exponents for the mixture components
   *
   * @return Boolean value: true if the threshold is crossed, false otherwise
   */
  int gas_passes_threshold(real t1, real t2, real threshold, real lambda,
                           vector gamma) {
    return gas_curve(t1, lambda, gamma) > threshold &&
           gas_curve(t2, lambda, gamma) <= threshold;
  }
}

data {
  int      M ;    // number of observations
  real    gas[M]; // tracer gas quantity (GAS)
  real    cevgm[M]; // cumulative expired volume of gas mixture (CEVGM)
  real    cevtg[M]; // cumulative expired volume of tracer gas (CEVTG)
  int      k[M]; // breath index
}

transformed data {
  int      nmax ;
  real    cevgm_tf[M - 1];
  real    cevtg_tf[M - 1];

  // Resolution for line search used to determine the real-valued stopping
  // 'breath'.
  nmax = 100;

  // Transform cumulative data to log increment scale.
  for (m in 1:(M - 1)) {
    cevgm_tf[m] = log(cevgm[m + 1] - cevgm[m]);
    cevtg_tf[m] = log(cevtg[m + 1] - cevtg[m]);
  }
}

parameters {
  // GAS curve.
  real<lower=0, upper=1> lambda; // a.k.a. gamma0
  positive_ordered[2]      gamma;
  real<lower=0>            error_gas;

  // CEVGM curve.
  real<lower=0>            alpha;
  real<lower=0>            error_cevgm;
}

```

mbw_individual_diffuse.stan

```

// CEVTG curve.
real<lower=0>      beta0;
real<lower=0>      beta1;
real<lower=0>  error_cevtg;
}

transformed parameters {
    // Stopping breaths.
    real<lower=0>  m_stop_40;
    real<lower=0>  m_stop_40_cont;

    // MBW quantities using standard stopping breath.
    real<lower=0>  lci40;
    real<lower=0>  cev40;

    // MBW quantities using model-based stopping breath.
    real<lower=0>  lci40_cont;
    real<lower=0>  cev40_cont;

    // Define MBW quantities from model parameters.
    // Use a threshold of 1/40 (= 0.025) for the gas concentration.
    for (m in 2:100) {
        if (gas_passes_threshold(m - 1, m, 0.025, lambda, gamma)) {
            // Use the standard stopping breath, k(40).
            m_stop_40 = m;
            cev40 = alpha * m_stop_40;
            lci40 = cev40 / beta0; // n.b. FRC = beta0

            // Use the model-based stopping 'breath', theta.
            // This stopping breath is real-valued rather than integer-valued.
            // It is determined by a simple line search.
            for (i in ((m - 1) * nmax):(m * nmax)) {
                if (gas_passes_threshold(1.0 / nmax * (i - 1),
                                         1.0 / nmax * i, 0.025, lambda, gamma)) {
                    m_stop_40_cont = 1.0 / nmax * i;
                    cev40_cont = alpha * m_stop_40_cont;
                    lci40_cont = cev40_cont / beta0; // n.b. FRC = beta0
                }
            }
        }
    }
}

model {
    // Declare local variables.
    // These are used to store the mean and sd of the 3 curves, see below.
    vector[M]      gas_mean;
    vector[M - 1]  cevgm_mean;
    vector[M - 1]  cevtg_mean;
    vector[M]      gas_sd;
    vector[M - 1]  cevgm_sd;
    vector[M - 1]  cevtg_sd;

    // Priors (diffuse).

    lambda ~ beta(2, 2); // a.k.a. gamma0
    gamma[1] ~ normal(0, 10);
    gamma[2] ~ normal(0, 10);

    beta0 ~ normal(0, 1000);
    beta1 ~ normal(0, 10);

    alpha ~ normal(0, 100);

    error_gas ~ cauchy(0, 2.5);
    error_cevgm ~ cauchy(0, 2.5);
    error_cevtg ~ cauchy(0, 2.5);
}

```

mbw_individual_diffuse.stan

```
// Calculate the mean and sd of the 3 curves.
for (m in 1:M) {
  gas_mean[m] = gas_curve(k[m], lambda, gamma);
  gas_sd[m]   = error_gas;
}
for (m in 1:(M - 1)) {
  cevqm_mean[m] = log(alpha);
  cevtg_mean[m] = log(beta0) + log(1 - exp(-beta1)) - (beta1 * (k[m]));
  cevqm_sd[m] = error_cevqm;
  cevtg_sd[m] = error_cevtg;
}

// Define the probability models for the 3 curves.
gas      ~ lognormal(log(gas_mean),   gas_sd);
cevqm_tf ~ normal(  cevqm_mean , cevqm_sd);
cevtg_tf ~ normal(  cevtg_mean , cevtg_sd);
}
```

mbw_individual_informative.stan

```

functions {
  /**
   * Evaluate the tracer gas quantity at a particular time point.
   * This is a two-component exponential decay model.
   *
   * @param t      Time point at which to evaluate the gas quantity
   * @param lambda Mixture weight parameter (a.k.a. gamma0)
   * @param gamma  Exponents for each component
   *
   * @return Gas quantity (between 0 and 1) at the given time point.
   */
  real gas_curve(real t, real lambda, vector gamma) {
    return lambda * exp(-gamma[1] * t) + (1 - lambda) * exp(-gamma[2] * t);
  }

  /**
   * Determine if the tracer gas quantity crosses a given threshold between
   * two time points, t1 and t2.
   *
   * @param t1      First time point (left end of desired time interval)
   * @param t2      Second time point (right end of desired time interval)
   * @param threshold Threshold for the gas quantity
   * @param lambda  Mixture weight parameter (a.k.a. gamma0)
   * @param gamma   Exponents for the mixture components
   *
   * @return Boolean value: true if the threshold is crossed, false otherwise
   */
  int gas_passes_threshold(real t1, real t2, real threshold, real lambda,
                           vector gamma) {
    return gas_curve(t1, lambda, gamma) > threshold &&
           gas_curve(t2, lambda, gamma) <= threshold;
  }
}

data {
  int      M ;    // number of observations
  real    gas[M]; // tracer gas quantity (GAS)
  real    cevgm[M]; // cumulative expired volume of gas mixture (CEVGM)
  real    cevtg[M]; // cumulative expired volume of tracer gas (CEVTG)
  int      k[M]; // breath index
}

transformed data {
  int      nmax ;
  real    cevgm_tf[M - 1];
  real    cevtg_tf[M - 1];

  // Resolution for line search used to determine the real-valued stopping
  // 'breath'.
  nmax = 100;

  // Transform cumulative data to log increment scale.
  for (m in 1:(M - 1)) {
    cevgm_tf[m] = log(cevgm[m + 1] - cevgm[m]);
    cevtg_tf[m] = log(cevtg[m + 1] - cevtg[m]);
  }
}

parameters {
  // GAS curve.
  real<lower=0, upper=1> lambda; // a.k.a. gamma0
  positive_ordered[2] gamma;
  real<lower=0> error_gas;

  // CEVGM curve.
  real<lower=0> alpha;
  real<lower=0> error_cevgm;
}

```

mbw_individual_informative.stan

```

// CEVTG curve.
real<lower=0>      beta0;
real<lower=0>      beta1;
real<lower=0>  error_cevtg;
}

transformed parameters {
// Stopping breaths.
real<lower=0>  m_stop_40;
real<lower=0>  m_stop_40_cont;

// MBW quantities using standard stopping breath.
real<lower=0>  lci40;
real<lower=0>  cev40;

// MBW quantities using model-based stopping breath.
real<lower=0>  lci40_cont;
real<lower=0>  cev40_cont;

// Define MBW quantities from model parameters.
// Use a threshold of 1/40 (= 0.025) for the gas concentration.
for (m in 2:100) {
  if (gas_passes_threshold(m - 1, m, 0.025, lambda, gamma)) {
    // Use the standard stopping breath, k(40).
    m_stop_40 = m;
    cev40 = alpha * m_stop_40;
    lci40 = cev40 / beta0; // n.b. FRC = beta0

    // Use the model-based stopping 'breath', theta.
    // This stopping breath is real-valued rather than integer-valued.
    // It is determined by a simple line search.
    for (i in ((m - 1) * nmax):(m * nmax)) {
      if (gas_passes_threshold(1.0 / nmax * (i - 1),
                               1.0 / nmax * i, 0.025, lambda, gamma)) {
        m_stop_40_cont = 1.0 / nmax * i;
        cev40_cont = alpha * m_stop_40_cont;
        lci40_cont = cev40_cont / beta0; // n.b. FRC = beta0
      }
    }
  }
}

model {
// Declare local variables.
// These are used to store the mean and sd of the 3 curves, see below.
vector[M]      gas_mean;
vector[M - 1]   cevgm_mean;
vector[M - 1]   cevtg_mean;
vector[M]      gas_sd;
vector[M - 1]   cevgm_sd;
vector[M - 1]   cevtg_sd;

// Priors (informative).

lambda ~ normal(0.63, 0.18); // a.k.a. gamma0
gamma[1] ~ lognormal(log(0.12), 0.17);
gamma[2] ~ lognormal(log(0.40), 0.47);

beta0 ~ normal(126, 18);
beta1 ~ normal(0.136, 0.024);

alpha ~ normal(30, 6.5);

error_gas ~ normal(0.06, 0.020);
error_cevgm ~ normal(0.09, 0.026);
error_cevtg ~ normal(0.20, 0.047);
}

```

mbw_individual_informative.stan

```
// Calculate the mean and sd of the 3 curves.
for (m in 1:M) {
    gas_mean[m] = gas_curve(k[m], lambda, gamma);
    gas_sd[m]   = error_gas;
}
for (m in 1:(M - 1)) {
    cevgm_mean[m] = log(alpha);
    cevtg_mean[m] = log(beta0) + log(1 - exp(-beta1)) - (beta1 * (k[m]));
    cevgm_sd[m] = error_cevgm;
    cevtg_sd[m] = error_cevtg;
}

// Define the probability models for the 3 curves.
gas      ~ lognormal(log(gas_mean),   gas_sd);
cevgm_tf ~ normal(  cevgm_mean , cevgm_sd);
cevtg_tf ~ normal(  cevtg_mean , cevtg_sd);
}
```

lme_exchangeable_separate.stan

```

data {
  int<lower=0> n_all ; // number of observations
  int<lower=0> n_item; // number of participants (items)
  int<lower=0> n_meth; // number of methods
  real y[n_all]; // outcome variable
  int<lower=1> item[n_all]; // item index
  int<lower=1> meth[n_all]; // method index
}

transformed data {
  int<lower=1> n_factor;
  n_factor = n_all / n_meth;
}

parameters {
  // Parameters for each method.
  vector[n_meth] alpha; // mean effect
  vector[n_meth] sigma; // sd

  // Random effects due to item.
  vector[n_item] u_raw; // per-item random effect
  real<lower=0> gamma; // sd

  // Random effects due to interaction between items and methods.
  vector[n_item] c_raw[n_meth]; // per-combination random effect
  real<lower=0> tau ; // sd
}

model {
  vector[n_item] u ; // per-item random effect
  vector[n_item] c[n_meth]; // per-combination random effect

  // Prior for fixed components.
  alpha ~ normal(0, 10000);

  // Priors for variance components.
  gamma ~ cauchy(0, 2.5);
  sigma ~ cauchy(0, 2.5);
  tau ~ cauchy(0, 2.5);

  // Distributions of random effects.
  u_raw ~ normal(0, 1);
  u = gamma * u_raw;

  for (i in 1:n_meth) {
    c_raw[i] ~ normal(0, 1);
    c[i] = tau * c_raw[i];
  }

  // Distribution of the outcome variable.
  for (n in 1:n_all) {
    y[n] ~ normal(alpha[meth[n]] +
                  u[item[n]] +
                  c[meth[n], item[n]], +
                  sigma[meth[n]]);
  }
}

generated quantities {
  real<lower=0> sigmaRatio[2];
  real alphaDiff[2];

  sigmaRatio[1] = sigma[1] / sigma[2];
  sigmaRatio[2] = sigma[1] / sigma[3];

  alphaDiff[1] = alpha[1] - alpha[2];
  alphaDiff[2] = alpha[1] - alpha[3];
}

```

lme_linked_common.stan

```

data {
  int<lower=0> n_all ; // number of observations
  int<lower=0> n_item; // number of participants (items)
  int<lower=0> n_meth; // number of methods
  real y[n_all]; // outcome variable
  int<lower=1> item[n_all]; // item index
  int<lower=1> meth[n_all]; // method index
  int<lower=1> repl_ind[n_all]; // item-replicate index
}

transformed data {
  int<lower=1> n_factor;
  n_factor = n_all / n_meth;
}

parameters {
  // Parameters for each method.
  vector[n_meth] alpha; // mean effect
  vector[n_meth] sigma; // sd

  // Random effects due to item.
  vector[n_item] u_raw; // per-item random effect
  real<lower=0> gamma; // sd

  // Random effects due to interaction between items and methods.
  vector[n_item] c_raw[n_meth]; // per-combination random effect
  real<lower=0> tau ; // sd

  // Random effects due to interaction between items and replicates.
  vector[n_factor] a_raw; // item-replicate interaction effect
  real<lower=0> omega; // sd
}

model {
  vector[n_item] u ; // per-item random effect
  vector[n_item] c[n_meth]; // per-combination random effect
  vector[n_factor] a ; // item-replicate interaction effect

  // Prior for fixed components.
  alpha ~ normal(0, 10000);

  // Priors for variance components.
  gamma ~ cauchy(0, 2.5);
  sigma ~ cauchy(0, 2.5);
  tau ~ cauchy(0, 2.5);
  omega ~ cauchy(0, 2.5);

  // Distributions of random effects.
  u_raw ~ normal(0, 1);
  u = gamma * u_raw;

  for (i in 1:n_meth) {
    c_raw[i] ~ normal(0, 1);
    c[i] = tau * c_raw[i];
  }

  for (i in 1:n_factor) {
    a_raw[i] ~ normal(0, 1);
    a[i] = omega * a_raw[i];
  }

  // Distribution of the outcome variable.
  for (n in 1:n_all) {
    y[n] ~ normal(alpha[meth[n]] +
                  u[item[n]] +
                  a[repl_ind[n]] +
                  c[meth[n], item[n]],
                  sigma[meth[n]]);
  }
}

```

lme_linked_common.stan

```
    }  
}  
  
generated quantities {  
    real<lower=0>  sigmaRatio[2];  
    real           alphaDiff[2];  
  
    sigmaRatio[1] = sigma[1] / sigma[2];  
    sigmaRatio[2] = sigma[1] / sigma[3];  
  
    alphaDiff[1]  = alpha[1] - alpha[2];  
    alphaDiff[2]  = alpha[1] - alpha[3];  
}
```